Review Article

The imaging spectrum and nuances of intrahepatic cholangiocarcinoma: a narrative review

Alexander Solomon Jung[1,2]^, Kevin Chialing Choong[3]^

[1]City of Hope National Medical Center, Duarte, CA, USA; [2]Department of Diagnostic Radiology, Helford Clinical Research Hospital, Duarte, CA, USA; [3]Department of Surgery, Division of Surgical Oncology, Helford Clinical Research Hospital, Duarte, CA, USA

Contributions: (I) Conception and design: AS Jung; (II) Administrative support: AS Jung; (III) Provision of study materials or patients: Both authors; (IV) Collection and assembly of data: Both authors; (V) Data analysis and interpretation: AS Jung; (VI) Manuscript writing: Both authors; (VII) Final approval of manuscript: Both authors.

Correspondence to: Alexander Solomon Jung, MD. City of Hope National Medical Center, Duarte, CA, USA. Email: ajung@coh.org.

Objective: To present the imaging spectrum and nuances of intrahepatic cholangiocarcinoma (IHCC), with particular emphasis on mass-forming IHCC and its evaluation with magnetic resonance imaging (MRI) and multidetector computed tomography (MDCT).

Background: The rationale for this review is the importance of optimal imaging evaluation throughout the diagnosis and management of each patient with IHCC.

Methods: PubMed was searched using the terms "intrahepatic cholangiocarcinoma imaging" from 2000 to February 2021, with the search then focused to the radiology literature. Surgical oncology and pathology literature pertinent to the discussion were also referenced.

Conclusions: The authors' intention is that this review will serve as a valuable resource for medical professionals with interest in the imaging of IHCC. A major portion of this review is a presentation of the typical and atypical imaging features of IHCC with histopathologic explanations for these features, and the potential overlap of these features with other tumors including atypical HCC and combined HCC-CC. The roles of serum tumor markers and tissue diagnosis as potential differentiators between imaging mimics are discussed. The imaging techniques that are most commonly utilized in IHCC characterization and disease extent determination, and their advantages and limitations are presented. The review concludes with a discussion of the clinicoprognostic implications of particular morphologic and contrast enhancement characteristics of IHCC.

Keywords: Cholangiocarcinoma (CC); intrahepatic cholangiocarcinoma (IHCC); diagnostic imaging; radiology

Received: 22 February 2021; Accepted: 04 June 2021; Published: 30 September 2021.

doi: 10.21037/dmr-21-20

View this article at: https://dx.doi.org/10.21037/dmr-21-20

Classification

IHCC accounts for 10–15% of primary liver tumors, is the second most common primary liver tumor after hepatocellular carcinoma (HCC), and has rising incidence and mortality worldwide (1). Classified by site of origin, intrahepatic cholangiocarcinoma (IHCC) is cholangiocarcinoma (CC) which arises in the liver parenchyma from a second-order/segmental or more peripheral bile duct (2,3). This is differentiated from extrahepatic CC which has perihilar and distal subtypes, with perihilar CC originating from a first-order duct (right and left hepatic ducts or the biliary bifurcation). Relative prevalences are perihilar (70%), distal (20%) and intrahepatic (10%) (4). From a surgical perspective,

^ ORCID: Alexander Solomon Jung, 0000-0001-9682-9478; Kevin Chialing Choong, 0000-0002-6521-7695.

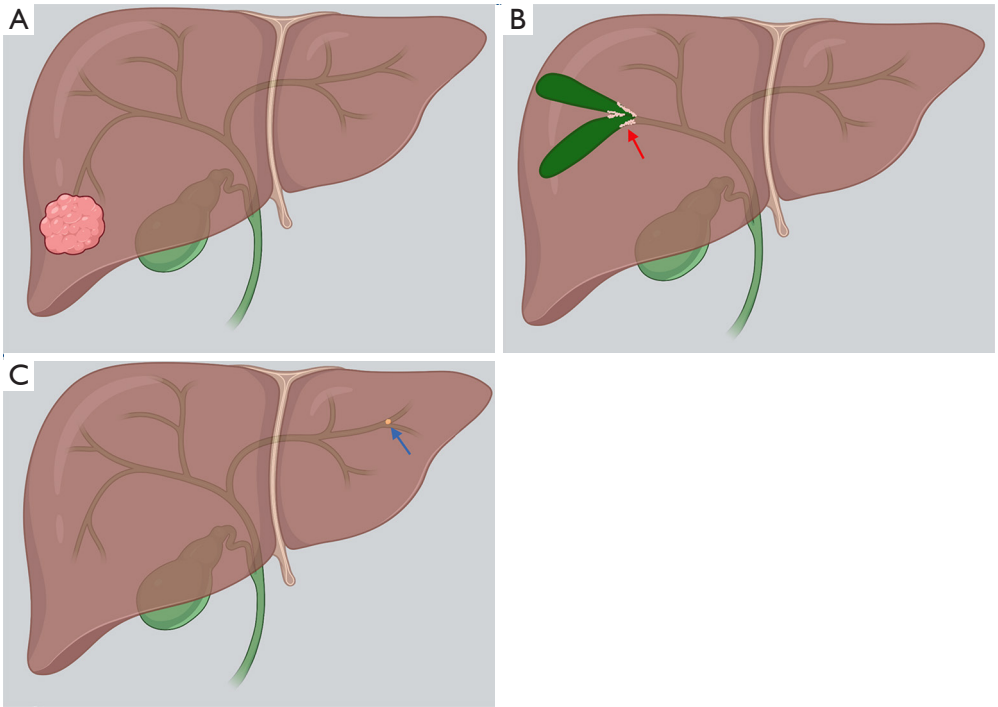

Figure 1 Types of IHCC. (A) Mass-forming IHCC grows with distinct borders. (B) Periductal infiltrating IHCC is characterized by tumor infiltration along the bile duct (red arrow) leading to proximal biliary dilatation. (C) Intraductal IHCC (blue arrow) is characterized by intraluminal papillary or granular growth within the bile duct. IHCC, intrahepatic cholangiocarcinoma.

perihilar CC is defined as tumor requiring resection of the confluence of the bile duct and may include perihilar tumors with a significant intrahepatic component. Management for resectable distal CC involves pancreaticoduodenectomy (4).

Classified by morphologic growth pattern, the most common type of IHCC is mass-forming, which is the focus of this review. The periductal and intraductal types are more common in perihilar and distal CC, but IHCC may also present in these forms (*Figure 1*). Periductal infiltrating type refers to stricture with scar-like fibrosis and intraductal growing type refers to intraluminal polypoid or cast-like lesions. Mixed type refers to periductal growth that progresses to a mass-forming plus periductal type, considered to have a worse prognosis than the mass-forming type (4). Interestingly, microscopic tumor spread beyond the macroscopic tumor varies by type of spread, greater with mucosal than submucosal extension. As such, the recommendation is made to resect further from the ends of macroscopic tumor in the mass-forming and intraductal types than the periductal type (4).

Management for resectable IHCC includes resection of the involved lobe or segments, with the goal an R0 (negative margin) resection while leaving an adequate liver remnant (1,5). Extrahepatic disease, including lymph node metastases beyond the regional basin (i.e., the regional N1 hilar, periduodenal and peripancreatic nodes), is a contraindication to resection. Bilateral multifocal or multicentric intrahepatic disease is also a contraindication to resection (5). Unfortunately, only 15% of patients present with resectable disease (1). We present the following article in accordance with the Narrative Review reporting checklist (available at https://dx.doi.org/10.21037/dmr-21-20).

Imaging features

On magnetic resonance imaging (MRI) and multidetector CT (MDCT), the morphology of mass-forming IHCC is typically a large mass, hyperintense to liver on T2-weighted MRI images, with an irregular-lobular margin and dilatation of adjacent intrahepatic ducts. Associated findings may include capsular retraction, satellite nodules and intrahepatic metastases, dilatation and thickening of peripheral intrahepatic ducts and vascular encasement usually without the formation of grossly visible tumor thrombus (unlike HCC). Calcification is rare.

Periductal type IHCC is associated with segmental dilatation of bile ducts containing bile having signal/attenuation similar to water unless secondary stones or sludge is present. Intraductal type is associated with segmental or lobar dilatation of intrahepatic ducts with bile having signal/attenuation different than water; an obstructing lesion may occasionally be seen (6).

Contrast enhancement characteristics of mass-forming IHCC vary. The most typical pattern is hypoenhancement of the majority of the mass with the exception of rim enhancement on arterial and portal venous phase images. Peripheral components demonstrating early enhancement and subsequent washout are considered to indicate areas of active growth (2,4). Delayed phase enhancement of the initially hypoenhancing central component is common with pure extracellular contrast agents (for both MRI and MDCT). This late enhancement is closely related to the amount of interstitial space in the often abundant fibrous stroma within the adenocarcinoma, and results in the apparent centripetal progression of enhancement (2,4).

Unlike the pure extracellular contrast agents, the MRI contrast agent gadoxetate disodium (Gd-EOB-DTPA, Bayer, New Jersey) has a biphasic mechanism of action—initial distribution in the extracellular space and then selective uptake by functioning hepatocytes and biliary excretion through the organic anionic transporting polypeptide (OATP8). In patients with preserved liver function, hepatic uptake can be evident at 20 minutes and lasts for several hours (i.e., the hepatobiliary phase). Mass-forming IHCC is usually heterogeneously hypointense to liver parenchyma in the hepatobiliary phase due to the absence of uptake (7).

A hepatobiliary phase target appearance has also been described when utilizing this contrast agent—comprised of central hyperintensity less than surrounding liver parenchyma (i.e., "gadoxetic acid cloud," reflecting intratumoral fibrosis) with peripheral rim hypointensity (4,7).

Atypical patterns of enhancement of mass-forming IHCC include homogenous hypervascular enhancement (HCC-like, more common in small lesions), prolonged enhancement, central necrosis (non-enhancing, more common in metastatic adenocarcinoma) and a mucinous variant with centripetal enhancement (continuous ragged rim enhancement as opposed to the stronger and globular enhancement of cavernous hemangioma) (2).

Imaging mimics

The imaging differential diagnosis for mass-forming IHCC includes HCC with cirrhotic stroma, sclerosing HCC, and combined hepatocellular carcinoma-cholangiocarcinoma (cHCC-CC) in patients with chronic liver disease, tumors with abundant fibrous stroma, immature abscesses, metastases and hepatic tuberculosis (2).

Atypical forms of IHCC and HCC can mimic each other. While most mass-forming IHCC can be accurately classified per the Liver Imaging Reporting and Data System (LI-RADS) as LR-M (probably or definitely malignant but not HCC specific), some atypical, particularly smaller CCs can be characterized as LR-5 or LR-4 (definitely or probably HCC, respectively), based on the presence of predominant (HCC-like) arterial hyperenhancement related to larger cellular components and less central stroma (4,8). A feature which may be helpful in distinguishing predominantly arterial-enhancing IHCC from HCC is the absence of contrast washout in the delayed phase of extracellular contrast agent-enhanced MRI (4). Scirrhous HCCs may have IHCC-like features, including an ill-defined margin, hepatic capsular retraction, progressive enhancement and the target appearance at hepatobiliary phase imaging (4).

Biphenotypic, cHCC-CC is a rare tumor which usually develops in conditions commonly found in patients with HCC or IHCC such as cirrhosis and hepatitis virus infection (5). It may mimic both HCC and CC, but has been reported to be more commonly misdiagnosed as CC than HCC. Features reported to favor cHCC-CC over CC include: tumors with an irregular shape, strong rim enhancement during the arterial phase, absence of the target appearance on hepatobiliary phase images, presence of major vascular thrombosis, and absence of intrahepatic bile duct dilatation (4).

Mimics of periductal infiltrating CC include stricturing inflammatory conditions such as primary and secondary sclerosing cholangitis, granulomatous and xanthogranulomatous cholangitis. Mimics of intraductal growing CC include intrabiliary metastases (9).

Tissue diagnosis

Given potential overlap in the imaging characteristics of mass-forming IHCC and other tumors, percutaneous image-guided needle biopsy may be considered for pathologic diagnosis, with the associated risk of complications such as bleeding and tract seeding, and the potential for sampling error and indeterminate biopsy. Another option is endoscopic biopsy if technically feasible.

Though these options are available, an American Hepato-Pancreato-Biliary Association-sponsored expert consensus statement in 2015 concluded that biopsy is not routinely recommended or necessary in all patients with suspected IHCC which is considered resectable. However, biopsy and pathologic diagnosis are considered necessary before systemic or locoregional therapies are initiated (5). When biopsy is obtained, immunostains are required to differentiate IHCC from metastatic lesions and from mixed hepatocellular tumors (5).

For the at risk for HCC population, the LI-RADS version 2018 uptake suggests judicious use of liver mass biopsy if deemed warranted by multidisciplinary tumor board discussion primarily for lesions which are suspicious for malignancy but not LR-5 (e.g., LR-4 or LR-M). LR-5 lesions do not generally require histologic confirmation prior to management, but biopsy of LR-5 lesions can be considered if: (I) the patient is not considered at high risk for HCC development, (II) the patient has an elevated carbohydrate antigen 19-9 (CA 19-9) level (described below) or carcinoembryonic antigen (CEA) level or another primary malignancy that can metastasize to liver, (III) confirmation of an HCC metastasis could change clinical decision-making, or (IV) biopsy may facilitate molecular characterization or is needed for clinical trial (8).

Tumor markers

CA 19-9, α-fetoprotein (AFP) and CEA are a routine part of preoperative liver mass characterization. Serum tumor markers tend to have low sensitivity but relatively high specificity for IHCC and HCC. CA 19-9 has 50% sensitivity and 75–90% specificity for IHCC at a level >100 U/mL. AFP is considered positive for HCC at a level >20 ng/mL, but can be negative in up to 40% of patients with HCC. cHCC-CC may demonstrate elevations of AFP and CA 19-9 (1,5) (*Table 1*).

Imaging modalities and scan techniques

The primary imaging modalities for IHCC include contrast-enhanced MRI with magnetic resonance cholangiopancreatography (MRCP) and contrast-enhanced MDCT.

MRI with MRCP is increasingly performed for CC. MRI pulse sequences include T1 in and out-of-phase, T2 in the axial and coronal planes, diffusion weighted (low B-value 0–200 sec/mm^2 and high B-value 800–1,000 sec/mm^2), precontrast and dynamic 3D T1-weighted post-contrast (arterial, portal and equilibrium phases), and 2D and 3D heavily T2-weighted MRCP sequences which are aligned to the common bile duct. Multiplanar reformatted (MPR) and maximum intensity projection (MIP) post-processed images of the biliary tree are generated from the 3D MRCP sequence. Thick slab 2D images (typically 4-8 cm thickness) are acquired during breath holds and less prone to motion, but pathologies such as intraductal lesions may be masked by partial volume averaging. Isotropic 3D MRCP images are acquired during free breathing and respiration- or navigator-triggered; they require a longer acquisition time and are more susceptible to motion artifacts (7).

Gadoxetic acid-enhanced MRI (Gd-EOB-DTPA) offers improved sensitivity for the detection of daughter nodules and intrahepatic metastases, both poor prognostic factors, as the high signal intensity of the liver parenchyma on hepatobiliary phase images (20 minutes or later) and the concomitant lack of uptake by the tumors results in improved lesion conspicuity (3,4,7).

Biliary phase images (50 minutes or later) also known as contrast-enhanced MR cholangiography can also be acquired, but contrast opacification of the biliary tree is dependent on liver function, as excretion of Gd-EOB-DTPA is mediated by the same transporter responsible for bilirubin transport. Feng and colleagues demonstrated that at high total bilirubin levels (>22 μmol/L), biliary tract opacification by excreted contrast is reduced. The relative signal intensity of liver parenchyma is reduced during all phases of enhancement at high bilirubin levels. Additionally, at high bilirubin levels, the relative signal intensities of the abdominal aorta, portal vein and spleen are decreased on dynamic phases, but increased on (the later) hepatobiliary and biliary phases (10).

MDCT includes precontrast, arterial (20–30 s after the initiation of contrast injection), portal venous (25–30 s later) and delayed (3–5 minutes after initiation) phase post-contrast images. Precontrast images are helpful in the detection of intraductal stones and in differentiating stones and tumors, and delayed phase images helpful in the demonstration of the fibrous stroma of CC. These images combined with MPR and MIP post-processed images provide an evaluation of the primary tumor, its relationship to vascular structures such as the hepatic artery and portal vein, and the ability to detect metastases (2).

MRI and CT images can be utilized for volumetric analysis of the anticipated liver remnant, including the assessment for compensatory hypertrophy induced by portal

Table 1 Imaging features of IHCC and IHCC mimics

Tumor type	Imaging features	Tumor markers
Typical mass-forming IHCC	CT: Irregular lesion. Hypoenhancement of the majority of the mass with the exception of rim enhancement on arterial and portal venous phase images. Centripetal progression of enhancement on venous to delayed phases	CA 19-9 elevated in 50%
	MRI: T2-hyperintense, cloud-like central hyperintensity on hepatobiliary phase or heterogeneously hypointense to liver parenchyma on hepatobiliary phase	CEA elevated in 15–20%
	Associated findings: capsular retraction, satellite nodules, intrahepatic metastases, biliary dilatation. hepatobiliary phase target appearance with Gd-EOB-DTPA	
	Typically LR-M when LI-RADS classification is applied	
Typical HCC	CT: hypervascular pattern with arterial enhancement and washout during the portal venous phase	AFP >20 ng/mL considered positive, but 40% can have AFP less than this
	MRI: arterial enhancement, portal phase washout, rim/capsule enhancement may persist.	
	LR-5, LR-4 and LR-M	
Small and atypical IHCC	Homogenous arterial enhancement	May have elevated CA 19-9 and CEA
	Prolonged enhancement	
	Central necrosis (no central enhancement)	
	Absence of contrast washout on delayed phase MRI with an extracellular contrast agent may help to differentiate from HCC	
	LIRADS classification can be used for population at risk for HCC (LR-4, LR-M)	
Small and atypical HCC	Scirrhous HCC may have IHCC-like features such as ill-defined margins, capsular retraction, progressive enhancement, and target appearance	May have elevated AFP
	LIRADS classification can be used for population at risk for HCC (LR-4, LR-5, LR-M)	
cHCC-CC	Irregular shape, strong rim enhancement during arterial phase, absence of target appearance on hepatobiliary phase images, presence of major vascular thrombosis, and absence of intrahepatic biliary dilatation may favor cHCC-CC over IHCC	May have elevated AFP and CA 19-9
Metastasis	Variable depending on the tumor type, may be multiple Known or detectable primary malignancy	Tumor markers may be elevated depending on the primary tumor type

cHCC-CC, combined hepatocellular carcinoma-cholangiocarcinoma; IHCC, intrahepatic cholangiocarcinoma; MRI, magnetic resonance imaging; CEA, carcinoembryonic antigen; AFP, α-fetoprotein.

vein embolization (4).

Multidetector chest CT is acquired as part of the initial evaluation to exclude metastatic disease to the lungs (1).

Ultrasound can demonstrate IHCCs as masses of variable echogenicity and may also visualize associated biliary dilatation. However, ultrasound is less accurate for assessing disease burden and tumor resectability than MRI or MDCT (3).

The utility of fluorodeoxyglucose (F18) position emission tomography (PET-CT and PET-MRI) when no extrahepatic disease has been demonstrated on MDCT or MRI has been questioned. Some small studies have suggested however that FDG PET may result in the identification of occult metastatic disease in up to 20–30% of patients and may help to rule out an occult primary tumor (5).

Table 2 Advantages and limitations of imaging techniques for IHCC

Technique	Uses	Advantages	Limitations
Multidetector CT	Tumor characterization	Higher spatial resolution	Ionizing radiation
	Staging-resectability determination (including chest CT)	Faster acquisition, less susceptible to motion-related degradation	Potential contrast reaction
	Treatment response assessment	Allows for multiplanar reconstructed images and liver volumetrics	Potential contrast nephrotoxicity
	Detection of recurrent tumor		
MRI and MRCP	Tumor characterization	Higher tissue contrast	Longer acquisition. More susceptible to motion-related degradation and patient intolerance
	Staging-resectability determination	Multiparametric tumor assessment	Potential contrast reaction
	Treatment response assessment	Improved detection of intrahepatic metastases on hepatobiliary phase and diffusion-weighted images	Potential nephrogenic systemic fibrosis in at risk patients
	Detection of recurrent tumor	Allows for noninvasive visualization specifically of the biliary tree (MRCP and MR cholangiography)	Potential gadolinium deposition
		Allows for liver volumetrics	
		No ionizing radiation	
ERCP	Histologic confirmation	High spatial resolution for characterizing biliary strictures	Invasive
	Biliary decompression	Real-time visualization facilitating interventions such as brushings and stenting	Incomplete evaluation for upstream ducts in high grade biliary obstruction (4)
^{18}F-FDG PET-CT/ PET-MRI	Assessment for metastatic disease	Utility considered controversial in patients in whom MDCT and/or MRI have shown no extrahepatic disease, but may change management in a minority of cases by demonstrating occult metastases (1,3,5)	Limited utility for the specific diagnosis of IHCC
			False positive in biliary inflammation (4)
			False negative in mucinous IHCC (4)

IHCC, intrahepatic cholangiocarcinoma; MDCT, multidetector computed tomography; MRI, magnetic resonance imaging; ERCP, endoscopic retrograde cholangiopancreatography.

Invasive techniques include endoscopic retrograde cholangiopancreatography (ERCP), choledochoscopy and intraductal ultrasound. ERCP allows for tissue biopsy and biliary stent insertion (4). Ideally, MDCT and MRI/MRCP should be performed prior to stent placement.

Advantages and limitations of these techniques are summarized in *Table 2*.

Prognostic imaging features

The term "daughter" or "satellite" nodule is generally used for a small lesion near the dominant mass, with the implication that it has spread from the mass (11). Defining satellite lesions as distinct from the dominant mass but within the same segment, Baheti and colleagues found a statistically significant decline in survival in a retrospective study of 92 patients with IHCC who had single phase CT scans when comparing groups with the presence of a solitary tumor (median 33 months), tumor with adjacent nodules in the same liver segment (23 months), and multiple nodules beyond the segment of the primary tumor (14 months). Also found was an increasing tendency towards developing

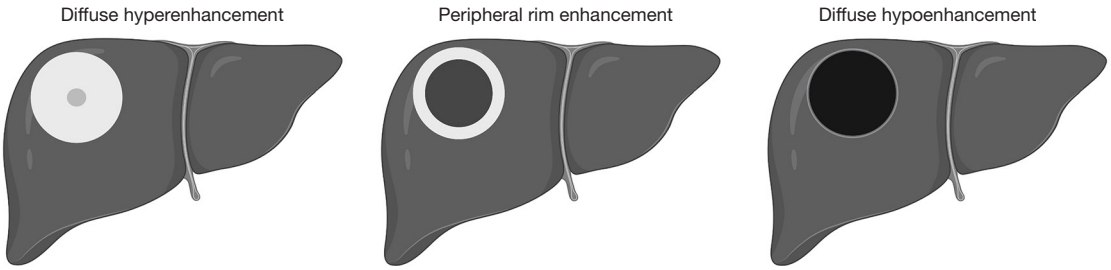

Figure 2 Arterial enhancement patterns of mass-forming IHCC. IHCC, intrahepatic cholangiocarcinoma.

distant metastases, both at presentation and subsequently, when moving from solitary tumor to satellite lesions and intrahepatic metastases (11).

In the same study Baheti and colleagues found the lungs (24%), peritoneum (18%) and bones (14%) to be the most common sites of distant metastasis (11). In an autopsy series by Nakajima and colleagues of 102 patients with CC, 71 with IHCC, the most common sites were the lungs, pancreas, bones and adrenal glands, with distant metastases seen in 83% of patients and nodal metastases in 86% (12).

In a retrospective study of 301 patients who underwent resection of IHCC with curative intent, 81.1% with R0 resection, Hyder and colleagues found that during a median follow-up of 31 months, 53.5% of patients developed a recurrence, defined as either biopsy-proven CC or lesions suspicious on imaging with an elevated CA 19-9 level. The median recurrence-free survival (RFS) was 20.2 months, 5-year disease-free survival 32.1% and median overall survival (OS) 37.8 months. The most common site for initial recurrence was intrahepatic (60.9%), followed by extrahepatic recurrence (21%) and simultaneous intra- and extrahepatic disease (18.6%) (13).

Recent studies suggest that the enhancement characteristics of mass-forming IHCC correlate with prognosis. In a retrospective study of 32 patients who underwent multiphase CT, Asayama and colleagues found that the group of patients with tumors in which more than 2/3 of the mass demonstrated delayed phase enhancement had a lower survival than the group with less than 2/3 delayed phase enhancement. The amount of delayed phase enhancement showed a statistically significant correlation with the amount of fibrous stroma and frequency of perineural invasion on histopathology (14).

In a retrospective study of 134 patients who had preoperative gadoxetic acid-enhanced MRI, Min and colleagues found that the arterial phase enhancement pattern of the tumor was an independent prognostic factor for risk of death and recurrence following resection (15). Arterial phase (20–35 s) hyperenhancement was defined as comprising more than 70% of the tumor surface (*Figure 2*). The 1-, 3- and 5-year death rates were 0%, 5.9% and 5.9% for the diffuse hyperenhancement group, 12.5%, 38.5% and 59.2% for the peripheral rim enhancement group and 30.3%, 67.7% and 87.9% for the diffuse hypoenhancement group. The 1-, 3- and 5-year recurrence rates were 15.0%, 25.6% and 25.6% in the diffuse hyperenhancement group, 36.4%, 59.0% and 79.4% in the peripheral rim enhancement group, and 71.7%, 85.1% and 85.1% in the diffuse hypoenhancement group. Patients with tumors demonstrating diffuse arterial hyperenhancement had more frequent chronic liver disease (65%), less frequent vascular invasion (30%), less frequent tumor necrosis (15%) and smaller tumor size (median size 2.6 cm, 1.5–8.0 cm) at histopathology than the other two groups (15).

Along the same lines, in a retrospective study by Choi and colleagues of patients who underwent surgical resection for primary liver cancers, 97 surgically proven HCCs were included in the matched control group, and 61 and 86 surgically proven IHCCs and combined HCC-CCs were included in the study cohort (16). LI-RADS categories were assigned to these masses based on review of gadoxetic acid-enhanced MRIs. For IHCC, 84% were categorized as LR-M, 2% as LR-4 and 5% as LR-5. For cHCC-CC, 28% were categorized as LR-M, 43.4% as LR-4 and 11% as LR-5, with these scores between those of HCC and IHCC. Median OS and RFS rates for cHCC-CC categorized as LR-M were similar to those for IHCC and lower than for HCC. The survival rate for cHCC-CC categorized as LR-4 or LR-5 did not significantly differ from HCC but was slightly higher than that of IHCC, though this was not statistically significant. Tumors

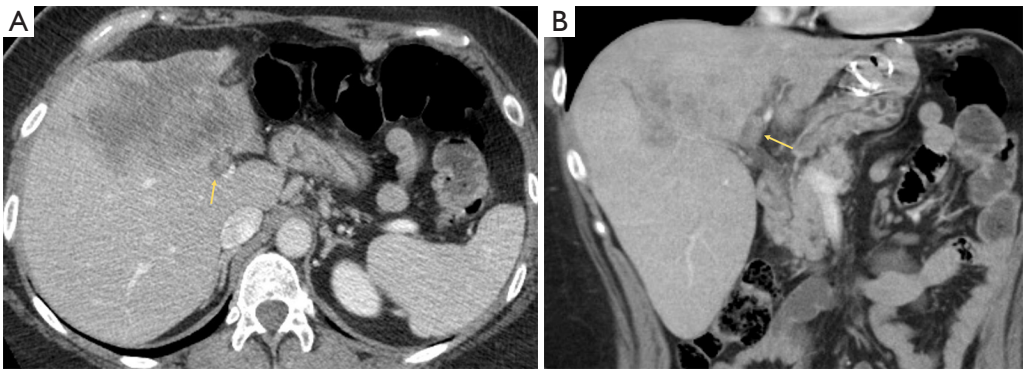

Figure 3 Axial (A) and coronal (B) portal venous phase MDCT images demonstrate a predominantly hypoenhancing liver parenchymal mass with an intraductal component (yellow arrows), a mixed type CC. Resection include extended left hepatectomy, bile duct excision and hepaticojejunostomy, with confirmed intraductal tumor. MDCT, multidetector computed tomography; CC, cholangiocarcinoma.

categorized as LR-M were associated with significantly poorer OS and RFS than those categorized as LR-4 or LR-5. At multivariate analysis, only the LI-RADS category showed an independent correlation with OS, while both LI-RADS category and pathologic diagnosis showed independent correlations with RFS (13). The implication was that though cHCC-CC may be difficult to differentiate from HCC at imaging, the post-surgical prognosis for these diseases is similar if MRI features used in the determination of LI-RADS scores are similar: better prognosis when MRI features resemble HCC (i.e., LR-4 or LR-5) and worse prognosis when features resemble IHCC (i.e., LR-M), suggesting that the LI-RADS score can serve as a prognostic imaging biomarker for primary liver cancers (16).

In a prospective study of 21 patients with unresectable IHCC refractory to standard chemotherapy who underwent yttrium-90 radioembolization therapy, Camacho and colleagues compared the ability of three imaging-based response criteria to predict OS—Response Evaluation Criteria in Solid Tumors (RECIST 1.1), a modified version of RECIST (mRECIST) and European Association for the Study of the Liver (EASL) (17). While RECIST is an overall tumor size-based assessment, the modification made to the mRECIST and EASL response criteria for this study was that size measurements were acquired of the delayed phase (180 s post-injection) enhancing components of the tumors, acknowledging the particular imaging characteristics of mass-forming IHCC. At 3 months post-radioembolization, target lesion objective response rates (including complete response and partial response) were 6.2% utilizing RECIST, 56.2% for mRECIST and 50% for EASL. Using mRECIST and EASL, satisfaction of criteria for target objective response at 3-month imaging was predictive of survival (median 21.4 months for responders versus 7.4 months for nonresponders using mRECIST, and 24.3 months versus 6.2 months for EASL). Utilizing RECIST, no statistically significant difference in survival between responders and nonresponders was observed at 3 months. The authors encouraged further investigation in larger cohorts with pathologic correlation for validation of these proposed IHCC locoregional therapy-focused modifications to imaging response criteria (17).

Image gallery

Illustrative MDCT and MRI-MRCP case examples are provided in an image gallery (*Figures 3-5*).

Summary

Accurate diagnosis, determination of disease extent to properly inform the choice of therapy, guidance to facilitate biopsy, assessment for treatment response, detection of disease progression and recurrence, and prognostic information are all meaningful goals of imaging IHCC. Knowledge of the spectrum of the imaging features and nuances of IHCC, their pathologic correlates and clinical significance, and the most optimal image techniques is crucial to achieving these goals. Further research to improve the ability of imaging to differentiate between mass-forming IHCC, HCC (particularly atypical and small HCC) and cHCC-CC is warranted.

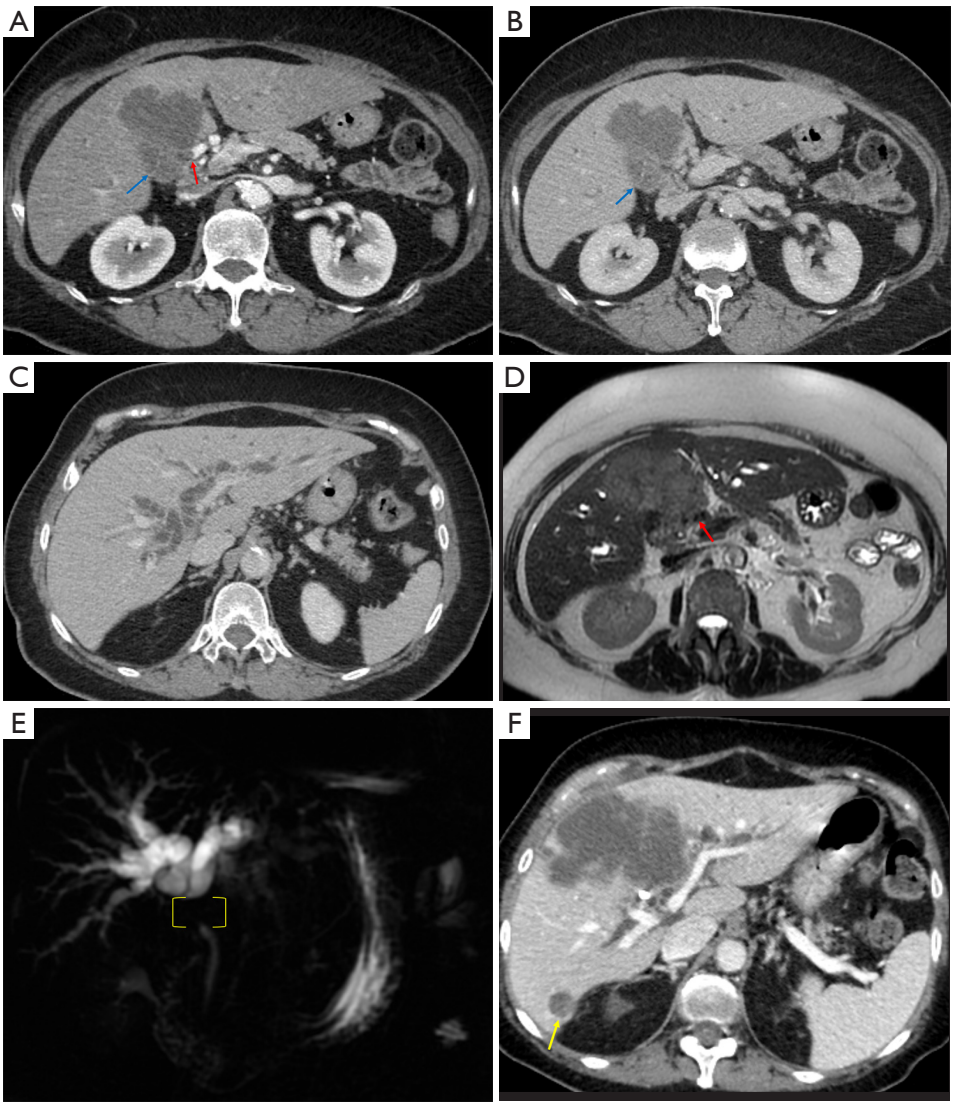

Figure 4 Unresectable left lobe IHCC due to hilar involvement. (A,B) Axial MDCT arterial and portal venous images demonstrate a predominantly hypoattenuating mass abutting the gallbladder (GB = blue arrow) with abutment of the hepatic artery (red arrow); delayed phase images (not shown) demonstrate similar mass attenuation. (C) Intrahepatic bile duct dilatation is superior/upstream to this mass. (D) Axial MRCP image demonstrates abnormality with signal essentially identical to the intrahepatic mass within the hepatic hilum encasing the right hepatic artery (red arrow). (E) Thick slab 2D MRCP image demonstrates the length of tumor-related stricture of the common duct (yellow brackets). (F) Despite chemotherapy, follow-up MDCT demonstrates tumor enlargement and a new metastasis in the right lobe (yellow arrow). Yttrium-90 transarterial radioembolization is planned. IHCC, intrahepatic cholangiocarcinoma; MDCT, multidetector computed tomography; MRCP, magnetic resonance cholangiopancreatography.

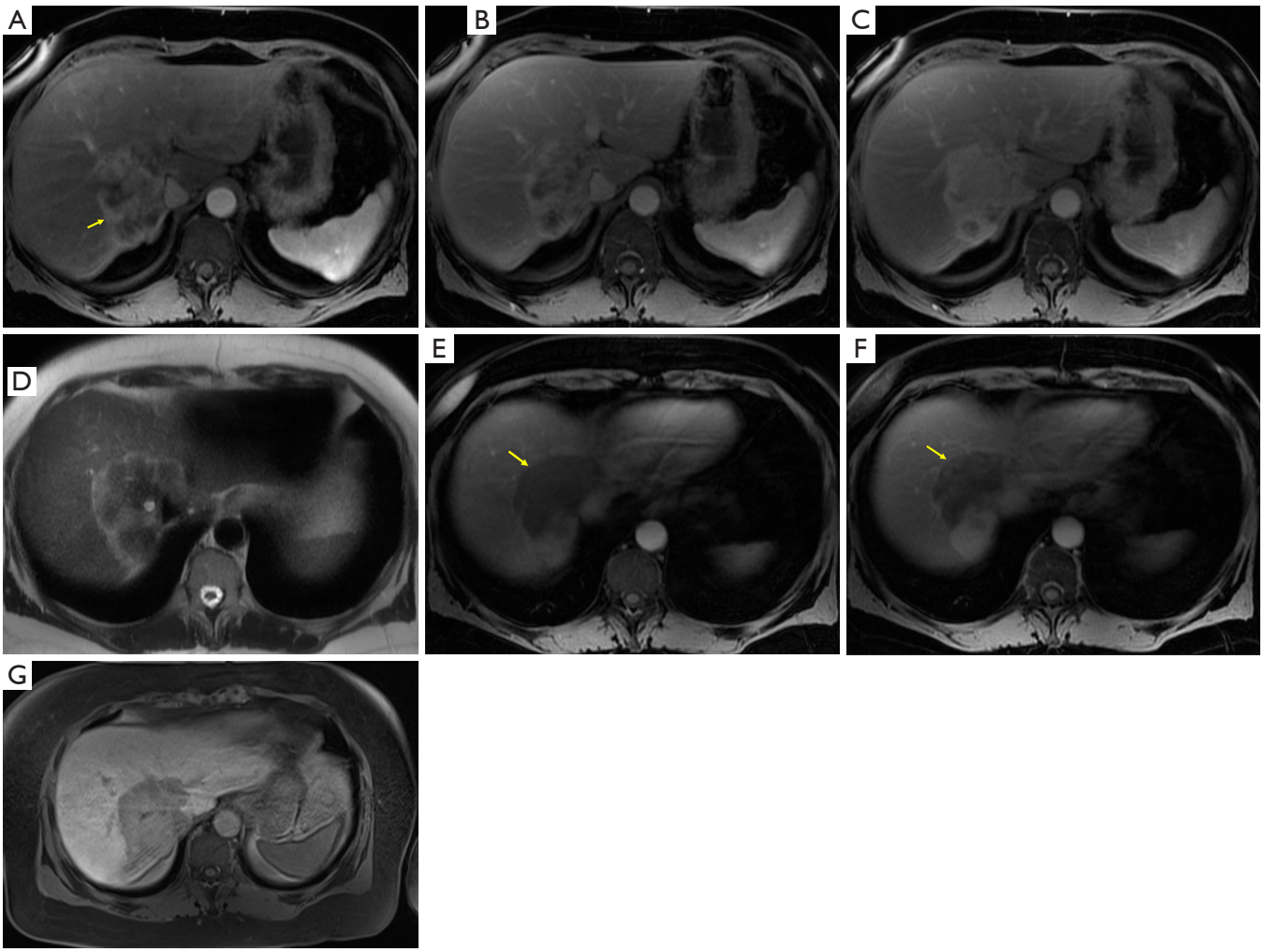

Figures 5 Different enhancement characteristics within a single IHCC. (A) Arterial phase MRI images demonstrate avid, heterogenous enhancement within the posteroinferior part of the tumor (yellow arrow). (B) Portal phase images demonstrate centripetally progressing enhancement. (C) 5-minute delayed images (extracellular contrast agent) demonstrate essentially complete persisting hyperenhancement, consistent with fibrous stroma. (D) T2-weighted images demonstrate heterogeneity throughout the mass. Unlike this component, a more superior component of the mass (yellow arrow) is predominantly hypoenhancing on all phases—arterial (E) and delayed images (F) shown. (G) 20 min delayed phase images acquired with the contrast agent Gd-EOB-DPTA demonstrate the hepatobiliary phase target sign with peripheral hypointensity and central hyperintensity ("gadoxetic acid cloud"). This mass is considered unresectable due to inferior vena caval, right and middle hepatic vein and right portal vein abutment. IHCC, intrahepatic cholangiocarcinoma.

Acknowledgments

Funding: None.

Footnote

Provenance and Peer Review: This article was commissioned by the Guest Editor (Yi-Jen Chen) for the series "Locoregional and systemic treatment in intrahepatic cholangiocarcinoma" published in *Digestive Medicine Research*. The article has undergone external peer review.

Reporting Checklist: The authors have completed the Narrative Review reporting checklist. Available at https://dx.doi.org/10.21037/dmr-21-20

Conflicts of Interest: Both authors have completed the

ICMJE uniform disclosure form (available at https://dx.doi.org/10.21037/dmr-21-20). The series "Locoregional and systemic treatment in intrahepatic cholangiocarcinoma" was commissioned by the editorial office without any funding or sponsorship. The authors have no other conflicts of interest to declare.

Ethical Statement: The authors are accountable for all aspects of the work in ensuring that questions related to the accuracy or integrity of any part of the work are appropriately investigated and resolved.

References

1. Mejia JC, Pasko J. Primary Liver Cancers: Intrahepatic Cholangiocarcinoma and Hepatocellular Carcinoma. Surg Clin North Am 2020;100:535-49.
2. Chung YE, Kim MJ, Park YN, et al. Varying appearances of cholangiocarcinoma: radiologic-pathologic correlation. Radiographics 2009;29:683-700.
3. Baheti AD, Tirumani SH, Rosenthal MH, et al. Diagnosis and management of intrahepatic cholangiocarcinoma: a comprehensive update for the radiologist. Clin Radiol 2014;69:e463-70.
4. Joo I, Lee JM, Yoon JH. Imaging Diagnosis of Intrahepatic and Perihilar Cholangiocarcinoma: Recent Advances and Challenges. Radiology 2018;288:7-13.
5. Weber SM, Ribero D, O'Reilly EM, et al. Intrahepatic cholangiocarcinoma: expert consensus statement. HPB (Oxford) 2015;17:669-80.
6. Han JK, Choi BI, Kim AY, et al. Cholangiocarcinoma: pictorial essay of CT and cholangiographic findings. Radiographics 2002;22:173-87.
7. Inchingolo R, Maino C, Gatti M, et al. Gadoxetic acid magnetic-enhanced resonance imaging in the diagnosis of cholangiocarcinoma. World J Gastroenterol 2020;26:4261-71.
8. Chernyak V, Fowler KJ, Kamaya A, et al. Liver Imaging Reporting and Data System (LI-RADS) Version 2018: Imaging of Hepatocellular Carcinoma in At-Risk Patients. Radiology 2018;289:816-30.
9. Menias CO, Surabhi VR, Prasad SR, et al. Mimics of cholangiocarcinoma: spectrum of disease. Radiographics 2008;28:1115-29.
10. Feng ST, Wu L, Cai H, et al. Cholangiocarcinoma: spectrum of appearances on Gd-EOB-DTPA-enhanced MR imaging and the effect of biliary function on signal intensity. BMC Cancer 2015;15:38.
11. Baheti AD, Tirumani SH, Shinagare AB, et al. Correlation of CT patterns of primary intrahepatic cholangiocarcinoma at the time of presentation with the metastatic spread and clinical outcomes: retrospective study of 92 patients. Abdom Imaging 2014;39:1193-201.
12. Nakajima T, Kondo Y, Miyazaki M, et al. A histopathologic study of 102 cases of intrahepatic cholangiocarcinoma: histologic classification and modes of spreading. Hum Pathol 1988;19:1228-34.
13. Hyder O, Hatzaras I, Sotiropoulos GC, et al. Recurrence after operative management of intrahepatic cholangiocarcinoma. Surgery 2013;153:811-8.
14. Asayama Y, Yoshimitsu K, Irie H, et al. Delayed-phase dynamic CT enhancement as a prognostic factor for mass-forming intrahepatic cholangiocarcinoma. Radiology 2006;238:150-5.
15. Min JH, Kim YK, Choi SY, et al. Intrahepatic Mass-forming Cholangiocarcinoma: Arterial Enhancement Patterns at MRI and Prognosis. Radiology 2019;290:691-9.
16. Choi SH, Lee SS, Park SH, et al. LI-RADS Classification and Prognosis of Primary Liver Cancers at Gadoxetic Acid-enhanced MRI. Radiology 2019;290:388-97.
17. Camacho JC, Kokabi N, Xing M, et al. Modified response evaluation criteria in solid tumors and European Association for The Study of the Liver criteria using delayed-phase imaging at an early time point predict survival in patients with unresectable intrahepatic cholangiocarcinoma following yttrium-90 radioembolization. J Vasc Interv Radiol 2014;25:256-65.

doi: 10.21037/dmr-21-20

Cite this article as: Jung AS, Choong KC. The imaging spectrum and nuances of intrahepatic cholangiocarcinoma: a narrative review. Dig Med Res 2021;4:53.